Variable selection in microbiome compositional data analysis

Antoni Susin[1], Yiwen Wang[2], Kim-Anh Lê Cao[2] and M. Luz Calle ⓘ[3,*]

[1]Mathematical Department, UPC-Barcelona Tech, 08028 Barcelona, Spain, [2]Melbourne Integrative Genomics, School of Mathematics and Statistics, The University of Melbourne, Parkville, VIC 3010, Australia and [3]Biosciences Department, Faculty of Sciences and Technology, University of Vic—Central University of Catalonia, Carrer de la Laura, 13, 08500 Vic, Spain

ABSTRACT

Though variable selection is one of the most relevant tasks in microbiome analysis, e.g. for the identification of microbial signatures, many studies still rely on methods that ignore the compositional nature of microbiome data. The applicability of compositional data analysis methods has been hampered by the availability of software and the difficulty in interpreting their results. This work is focused on three methods for variable selection that acknowledge the compositional structure of microbiome data: *selbal*, a forward selection approach for the identification of compositional balances, and *clr-lasso* and *coda-lasso*, two penalized regression models for compositional data analysis. This study highlights the link between these methods and brings out some limitations of the centered log-ratio transformation for variable selection. In particular, the fact that it is not subcompositionally consistent makes the microbial signatures obtained from *clr-lasso* not readily transferable. *Coda-lasso* is computationally efficient and suitable when the focus is the identification of the most associated microbial taxa. *Selbal* stands out when the goal is to obtain a parsimonious model with optimal prediction performance, but it is computationally greedy. We provide a reproducible vignette for the application of these methods that will enable researchers to fully leverage their potential in microbiome studies.

INTRODUCTION

High-throughput DNA sequencing has tremendously enhanced microbiome research by allowing a more precise quantification of microbiome composition in a given environment. However, microbiome data analysis is challenging as it involves high-dimensional structured multivariate and sparse data that are compositional (1–3). The compositional structure of microbiome data is mainly due to (i) biological reasons, like microbial competition, interactions or nutrient availability, (ii) technical artifacts, such as DNA sequencing, and (iii) data transformations, such as rarefaction or proportions.

Microbial ecosystems are extremely complex and interactions within and between bacterial species can profoundly impact microbiome composition in natural environments (4). Microorganisms compete with their neighbors for space and resources. While some microbial populations can thrive under favorable conditions and resources, this may induce a decline of other competing species. Microbiome analysis should try to capture these interrelated changes of microbial compositions.

After bioinformatic processing and quality control, microbiome abundance is quantified as the number of reads for each microbial species or taxa per sample. Since the total counts per sample are highly variable, data are often normalized, for example, by transforming read counts to proportions. Normalization enables meaningful comparisons between samples with different library sizes, but it does not prevent from the 'compositional effect', i.e. the fact that changes in the abundance of one taxon induce changes in the observed abundances of the other taxa. The compositional nature of proportions is evident since they are constrained by a constant sum equal to 1. However, it is important to emphasize that read counts, sometimes (inappropriately) called absolute abundances, are also compositional. Even though they are not explicitly restricted to a constant sum, they are constrained by sequencing depth that induces strong dependencies and thus spurious correlations among the number of reads for the different taxa (2). Indeed, read counts are not informative of the absolute abundance of the taxa in the environment and only provide a relative measure of abundance when compared to the abundance of other taxa.

The need for analytical methods able to handle the compositional nature of microbiome data has been increasingly recognized (1,2,5–7), but the use of compositional data

---

*To whom correspondence should be addressed. Tel: +34 93 886 1222; Fax: +34 93 885 6900; Email: malu.calle@uvic.cat

analysis (CoDA) methods is still far from being a common practice. This is particularly critical in the context of microbiome variable selection, a task that can be seriously affected by the compositional effect (8).

Commonly used methods for variable selection, such as *LEfSe* (9) and metagenomeSeq (10), as well as methods originally proposed for transcriptomics analysis, *edgeR* (11) and *DESeq2* (12), perform univariate hypothesis testing that ignores the multivariate nature of the microbiome by testing each variable independently. In addition to library size normalization, *edgeR* and *DeSeq2* algorithms include heuristics, such as trimming (13), to mitigate the compositional effect.

Popular multivariate approaches for microbiome analysis include *PERMANOVA* (14), analysis of similarities (15) or tests based on the Dirichlet–multinomial distribution (16) to detect association between microbiome composition and the outcome of interest. However, these methods are limited as they do not propose variable selection and thus do not give any insight into which specific microbial species are driving the association. Sparse partial least-squares discriminant analysis (17) was also proposed for multivariate variable selection, but with a focus on prediction rather than statistical inference.

In the CoDA framework, the methods *ANCOM* (18) and *ALDEx2* (19) explicitly account for the compositional nature of microbiome data, but they rely on univariate tests. Other CoDA approaches for microbiome variable selection combine principal balances (20) with phylogenetic information to infer clades that explain variation in microbiome abundance (21–23). Recently, Morton *et al.* (24) introduced a multinomial regression model for differential ranking analysis to identify candidate taxa for log-ratio analysis. Quinn and Erb (25) proposed a discriminatory balance analysis for the identification of two- and three-part balances.

In this paper, we focus on three CoDA methods for variable selection that share similar formulation as generalized linear models with specific constraints: (i) selection of microbial balances with *selbal* (26); (ii) penalized regression (27–29) on centered log-ratio (clr)-transformed data; and (iii) penalized regression with constraints (30,31).

Selbal was proposed by Rivera-Pinto *et al.* (26) and relies on the concept of compositional balance, a measure that compares the average abundances of two groups of microbial species. The second method, referred to as *clr-lasso*, is the most straightforward way of adapting penalized regression to compositional data by transforming the covariates with the clr transformation (32) and applying penalized regression. The third method, *coda-lasso*, performs penalized regression on a log-contrast regression model, as we further describe in the 'Materials and Methods' section. For the sake of simplicity, we describe both penalized regression methods with an L_1 norm penalty term.

The applicability of these methods in microbiome studies has been limited by the availability of software as well as the difficulty in interpreting their results. Thus, the aim of this paper is to apply and assess these methods, discuss their advantages and drawbacks and provide some hints for the interpretation of their results. We provide a new R implementation of *coda-lasso*, new graphical representations of microbial balances and a reproducible bookdown vignette for all methods. In the following, we introduce the concept of compositional balance and describe the three methods *selbal*, *clr-lasso* and *coda-lasso*. We apply and interpret the results obtained in two case studies and compare the performance of the three methods on some simulated scenarios.

MATERIALS AND METHODS

Log-contrast functions and compositional balances

A composition is defined as a vector of positive real numbers, $x = (x_1, \ldots, x_k)$, $x_i > 0$, that contains relative information. This includes the case of a constant total sum (known as closed composition), e.g. when x is a vector of proportions with $\sum x_i = 1$, but also the case of a non-constant total sum constraint (non-closed composition), when the number of reads is constrained by the DNA sequencer capacity. In a composition, the value of each component is not informative by itself and the relevant information is contained in the ratios between the components, or parts (33). In this context, two compositions that are proportional are compositionally equivalent. The scale invariance principle (32) states that any function used for the analysis of compositional data must be invariant for any element from the same compositionally equivalent class and thus must provide the same result when applied to two proportional compositions.

The simplest invariant function is given by the log ratio between two components, i.e.

$$f(x) = \log\left(\frac{x_i}{x_j}\right), \quad i, j \in \{1, \ldots, k\}. \quad (1)$$

A more general form of an invariant function suitable for CoDA is a log-contrast function defined as a linear combination of logarithms of the components, with the constraint that the sum of the coefficients is equal to zero:

$$f(x) = \sum_{i=1}^{k} a_i \log(x_i), \quad \text{with} \sum_{i=1}^{k} a_i = 0. \quad (2)$$

A compositional balance is a special kind of log-contrast function that extends the log ratio between two components to the log ratio between the mean abundances of two groups of components. Formally, a balance in the context of microbiome compositions is defined as follows. Let $X = (X_1, X_2, \ldots, X_k)$ be the microbial composition of k taxa. Among these, we consider two disjoint subgroups of taxa, groups A and B, with k_A and k_B taxa indexed by $I_A \subset \{1, \ldots, k\}$ and $I_B \subset \{1, \ldots, k\}$, respectively, that do not share taxa ($I_A \cap I_B = \emptyset$). The abundance balance between A and B, denoted by $\mathcal{B}(A, B)$, is defined as the log ratio between the geometric mean abundances of the two groups of taxa:

$$\mathcal{B}(A, B) = C \cdot \log \frac{\left(\prod_{i \in I_A} X_i\right)^{1/k_A}}{\left(\prod_{j \in I_B} X_j\right)^{1/k_B}}, \quad (3)$$

where C is a normalization constant equal to $\sqrt{(k_A \cdot k_B)/(k_A + k_B)}$.

Equivalently, a balance can be rewritten as the difference between the arithmetic means of the log-transformed variables of the two groups of variables:

$$\mathcal{B}(A, B) \propto \frac{1}{k_A} \sum_{i \in I_A} \log X_i - \frac{1}{k_B} \sum_{j \in I_B} \log X_j, \quad (4)$$

where the sign $\propto$ means proportional. A balance is a one-dimensional measure, or score, that summarizes the average log-transformed abundances of two groups of taxa. The larger the value of $\mathcal{B}(A, B)$, the larger the average log abundance of taxa in group A compared to the average log abundance of taxa in group B. A value of $\mathcal{B}(A, B) = 0$ corresponds to the same average log abundance of taxa in groups A and B.

Note that balances defined in Equation (3) are referred as isometric log ratios (34) and should not be interpreted as summated log ratios or amalgamation balances that are defined as the log ratio of the total abundance in each group [see (35) for a comparison of these measures].

Selbal

Rivera-Pinto *et al.* (26) proposed a method for the identification of microbial signatures that are predictive of a phenotype of interest. Unlike approaches that define biomarker signatures as a linear combination of individual markers, the microbial signature from *selbal* has the form of a balance between two groups of microbial taxa. *Selbal* seeks for the two groups of taxa A and B whose relative abundances or balance $\mathcal{B}(A, B)$ is most associated with the outcome of interest Y according to the following generalized linear model:

$$g(E(Y)) = \beta_0 + \beta_1 \mathcal{B}(A, B) + \gamma' Z, \quad (5)$$

where β_0 is the intercept, β_1 is the regression coefficient for the balance score, $Z = (Z_1, Z_2, \ldots, Z_r)$ are additional non-compositional covariates and γ is the vector of regression coefficients for Z. The algorithm is implemented for linear and logistic regression.

The optimal balance $\mathcal{B}(A, B)$ relies on the identification of taxa that belong to either group A or group B. The first step of *selbal* algorithm evaluates all possible pairs of taxa to select the pair whose balance is most associated with the response. Then, a forward selection process is performed where, at each step, a new taxon is added to the current balance, either in group A or in group B of the balance to improve the optimization criterion. The objective criterion is defined as the area under the receiver operating characteristic (ROC) curve (AUC) or the proportion of explained deviance for a binary response, and the mean squared error for a linear response. The algorithm stops when there is no remaining variable that improves the optimization criterion or when the maximum number of components in the balance, established with a cross-validation procedure, is reached. *Selbal* results can be interpreted in terms of microbial balances, an important concept in microbiome studies to describe dysbiosis—a microbial disturbance or imbalance between beneficial and pathogenic microbes, associated with most human disease processes (36,37).

Clr-lasso

Penalized regression is a powerful approach for variable selection in a high-dimensional setting. The estimates of regression parameters are shrunk toward zero by adding a penalized term in the loss function. Variables with a nonzero coefficient are selected as informative variables associated with the outcome variable. Different penalized regression methods exist: the lasso (L_1 norm) puts a constraint on the sum of the absolute values of the regression coefficients, ridge uses the L_2 norm and elastic net uses a linear combination of L_1 and L_2 norms for the penalty term (27,29). A straightforward way of adapting penalized regression methods for CoDA is to first project the compositional data to a Euclidean space, e.g. using the clr transformation:

$$\mathrm{clr}(x) = \mathrm{clr}(x_1, \ldots, x_k)$$
$$= \left(\log\left(\frac{x_1}{g(x)}\right), \ldots, \log\left(\frac{x_k}{g(x)}\right) \right), \quad (6)$$

where $g(x) = \left(\prod x_j\right)^{1/k}$ is the geometric mean of the composition.

Interestingly, the clr transformation can be formulated as

$$\mathrm{clr}(x) = \mathrm{clr}(x_1, \ldots, x_k)$$
$$= (\log(x_1) - M, \ldots, \log(x_k) - M), \quad (7)$$

where M is the arithmetic mean of the log-transformed values: $M = (1/k) \sum_j \log(x_j)$. Thus, the transformed components are restricted to have a sum equal to zero.

After clr transformation, penalized regression, whether lasso, ridge or elastic net, can be applied. Here, we consider a linear regression model with L_1 penalty, referred as *clr-lasso*.

For $(y_i, x_{1i}, \ldots, x_{ki})$, $i = 1, \ldots, n$, where y_i is the response and $\mathbf{x}_i = (x_{1i}, \ldots, x_{ki})$ is the composition of k taxa for sample i, *clr-lasso* is defined as

$$y_i = \beta_0 + \beta_1 \mathrm{clr}(x_{1i}) + \cdots + \beta_k \mathrm{clr}(x_{ki}) + \varepsilon_i. \quad (8)$$

The regression coefficients $\beta = (\beta_0, \ldots, \beta_k)$ are estimated to minimize

$$\sum_{i=1}^{n} (y_i - \beta_0 - \beta_1 \mathrm{clr}(x_{1i}) - \cdots - \beta_k \mathrm{clr}(x_{ki}))^2$$
$$\text{subject to } \sum_{j \geq 1} |\beta_j| < t \quad (9)$$

for a given constant t. This is equivalent to minimizing

$$\sum_{i=1}^{n} (y_i - \beta_0 - \beta_1 \mathrm{clr}(x_{1i}) - \cdots - \beta_k \mathrm{clr}(x_{ki}))^2 + \lambda \sum_{j \geq 1} |\beta_j|, \quad (10)$$

where λ is the penalization parameter. Lasso shrinks some of the regression coefficients to zero, resulting in variable selection of the components with non-null coefficients.

A drawback of this method is that the selection is applied on the clr-transformed variables, which makes interpretation challenging. Equation (8) can be equivalently written

as

$$y_i = \beta_0 + \beta_1 (\log(x_{1i}) - M_i) + \cdots + \beta_k(\log(x_{ki}) - M_i) + \varepsilon_i, \quad (11)$$

$$y_i = \beta_0 + \beta_1 \log(x_{1i}) + \cdots + \beta_k \log(x_{ki}) - M_i(\beta_1 + \cdots + \beta_k) + \varepsilon_i (12)$$

where $M_i = (1/k) \sum_j \log(x_{ji})$. Both Equations (11) and (12) show that the term M is still present, even after lasso penalization. In other words, although lasso penalization removes irrelevant variables from the regression model, all variables remain in the model through the geometric mean of the clr transformation, M. When M has a high variance, the power to detect real associations can be reduced and the false discovery rate may increase, as we will explore in our simulation study.

Coda-lasso

An alternative regression approach for CoDA is to consider a log-contrast model (38). This consists in a linear regression model that relates log-transformed covariates with the outcome in the form of a log-contrast function; i.e. the regression coefficients (except the intercept) have a zero-sum constraint, which ensures the scale invariance principle. Such model can be adapted to penalized regression for CoDA variable selection. In the context of microbiome studies, Lin *et al.* (30) proposed an optimization procedure for penalized linear log-contrast regression models and Lu *et al.* (31) extended the approach to generalized linear regression models.

Coda linear regression with lasso penalization is formulated as

$$y_i = \beta_0 + \beta_1 \log(x_{1i}) + \cdots + \beta_k \log(x_{ki}) + \varepsilon_i, \quad (13)$$

with constraint $\sum_{j \geq 1} \beta_j = 0$, where the regression coefficients $\beta = (\beta_0, \ldots, \beta_k)$ are estimated to minimize

$$\sum_{i=1}^{n} (y_i - \beta_0 - \beta_1 \log(x_{1i}) - \cdots - \beta_k \log(x_{ki}))^2 + \lambda \sum_{j \geq 1} |\beta_j| \quad \text{subject to} \quad \sum_{j \geq 1} \beta_j = 0. \quad (14)$$

The minimization process is performed in two iterative steps based on soft thresholding and projection [see (31) for a detailed description].

Because of the zero-sum constraint, the fitted regression model can be interpreted as a weighted balance between two groups of components, those with a positive coefficient and those with a negative coefficient, i.e. a log ratio between two weighted geometric means:

$$\beta_0 + \sum_{i \in I_+} \beta_i \log X_i - \sum_{i \in I_-} \alpha_i \log X_i = \beta_0 + s_\beta \log\left(\frac{g_+(X)}{g_-(X)}\right), \quad (15)$$

where $I_+ \subset \{1, \ldots, k\}$ and $I_- \subset \{1, \ldots, k\}$ are the indices of the positive and negative coefficients, respectively. The parameters are defined as $\alpha_i = -\beta_i$ for $\beta_i < 0$ and $s_\beta = \sum_{i \in I_+} \beta_i = \sum_{i \in I_-} \alpha_i$. The weighted geometric means are defined

as

$$g_+(X) = \exp\left(\frac{1}{s_\beta} \sum_{i \in I_+} \beta_i \log X_i\right),$$

$$g_-(X) = \exp\left(\frac{1}{s_\beta} \sum_{i \in I_-} \alpha_i \log X_i\right). \quad (16)$$

Method commonalities

Relationship between clr-lasso *and* coda-lasso. If we add the constraint $\sum_{j \geq 1} \beta_j = 0$ to the clr-linear model, the clr transformation cancels out, and *clr-lasso* is equivalent to *coda-lasso*:

$$E(y_i) = \beta_0 + \beta_1 \text{clr}(x_{1i}) + \cdots + \beta_k \text{clr}(x_{ki})$$

$$= \beta_0 + \beta_1(\log(x_{1i}) - M_i) + \cdots + \beta_k(\log(x_{ki}) - M_i)$$

$$= \beta_0 + \beta_1 \log(x_{1i}) + \cdots + \beta_k \log(x_{ki}) - M_i(\beta_1 + \cdots + \beta_k)$$

$$= \beta_0 + \beta_1 \log(x_{1i}) + \cdots + \beta_k \log(x_{ki}), \quad (17)$$

since $\beta_1 + \cdots + \beta_k = 0$.

Thus, when the regression coefficients are constrained to $\sum_{j \geq 1} \beta_j = 0$, the clr transformation is not required and only a log transformation is needed. The regression coefficients inform of the weight of the log-transformed components.

Relationship between selbal *and* coda-lasso. Similar to *coda-lasso*, *selbal* can be expressed as a log-contrast linear model since the sum of the regression coefficients is equal to zero:

$$E(Y) = \beta_0 + \beta_1 \mathcal{B}(A, B)$$

$$= \beta_0 + \beta_1 \left(\frac{1}{k_A} \sum_{i \in I_A} \log X_i - \frac{1}{k_B} \sum_{j \in I_B} \log X_j\right). \quad (18)$$

The difference is that the coefficients in *selbal* for the taxa in each group are all equal to β_1/k_A for taxa in group A and β_1/k_B for taxa in group B, where k_A and k_B are the number of taxa in groups A and B, respectively.

Toy example. The similarities and differences between the three methods can be illustrated with a toy example. Let us consider an example where two groups of taxa A and B have been selected for prediction of disease status (cases and controls). Group A is composed of OTU_1 and OTU_2 and group B of OTU_3, OTU_4 and OTU_5. The difference between *selbal* balance score and *coda-lasso* balance score is that *selbal* assigns the same weight to the variables that belong to each group (proportional to the number of variables in each group), while *coda-lasso* assigns different weights to the taxa. In this example, *selbal* balance score is given by

$$\frac{1}{2} \log(OTU_1) + \frac{1}{2} \log(OTU_2) - \frac{1}{3} \log(OTU_3)$$

$$- \frac{1}{3} \log(OTU_4) - \frac{1}{3} \log(OTU_5)$$

and *coda-lasso* balance score is

$$\beta_1 \log(OTU_1) + \beta_2 \log(OTU_2) + \beta_3 \log(OTU_3)$$
$$+ \beta_4 \log(OTU_4) + \beta_5 \log(OTU_5),$$

where β_1 and β_2 are positive coefficients and β_3, β_4 and β_5 are negative coefficients, and $\beta_1 + \beta_2 = -(\beta_3 + \beta_4 + \beta_5)$. For *clr-lasso*, the linear regression score is of the form

$$\beta_1 clr(OTU_1) + \beta_2 clr(OTU_2) + \beta_3 clr(OTU_3)$$
$$+ \beta_4 clr(OTU_4) + \beta_5 clr(OTU_5),$$

with no restriction on the regression coefficients. This is why, the solution of *clr-lasso* cannot be considered as a balance as the sum of the regression coefficients is not equal to zero.

Graphical representation

The graphical representation provided by *selbal* helps interpreting the results, as shown in Figure 1 for the above toy example. The balance score distribution for the controls (in blue) is centered around zero, which means that the average log abundance of group *A* and group *B* is similar. On the contrary, the balance score distribution for the cases (in red) is shifted toward positive values; i.e. cases are characterized by a balance with a larger average log abundance in group *A* than in group *B*.

Similar representation can be extended for *coda-lasso*, with taxa with a positive regression coefficient assigned to group *A* and those with a negative regression coefficient assigned to group *B*.

Implementation

Selbal algorithm is implemented as an R package available on GitHub (https://github.com/UVic-omics/selbal). *Clr-lasso* first requires a clr transformation [e.g. *clr( )* function in the R package *compositions* (39)]. Next, penalized regression can be implemented with the R package *glmnet* (40). An implementation in Matlab of *coda-lasso* is available in (31). We have developed a new implementation of *coda-lasso* in R where, similarly to *glmnet*, the parameter α specifies the ratio between L_1 and L_2 penalization in the elastic net regularization. It is available at https://github.com/UVic-omics/CoDA-Penalized-Regression. A seamless application of all methods on the case studies is available as a reproducible R bookdown vignette on our GitHub page: https://github.com/UVic-omics/Microbiome-Variable-Selection/.

Datasets

High-fat high-sugar diet in mice. The study was conducted by Dr Lê Cao at the University of Queensland Diamantina Institute to investigate the effect of diet in mice. C57/B6 female black mice were housed in cages (three animals per cage) and fed with a high-fat high-sugar diet (HFHS) or a normal diet. Stool sampling was performed at Days 0, 1, 4 and 7. Illumina MiSeq sequencing was used to obtain the 16S rRNA sequencing data. The sequencing data were then processed with QIIME 1.9.0. For our analysis, we considered Day 1 only (HFHS-day1). The OTU (operational taxonomy unit) table after OTU filtering included 558 taxa and 47 samples (24 HFHS diet and 23 normal diet). Both OTU and the taxonomy tables are available on our GitHub page.

Crohn's disease. The pediatric Crohn's disease (CD) study (41) includes 975 individuals from 662 patients with CD and 313 without any symptoms. The processed data, from 16S rRNA gene sequencing after QIIME 1.7.0, were downloaded from Qiita (42) study ID 1939. The abundance table was agglomerated to the genus level, resulting in a matrix with 48 genera and 975 samples, which is accessible at our GitHub page.

Simulation study

We evaluated the performance of the three microbiome selection methods according to different scenarios. To mimic as realistically as possible real microbiome data structures, the simulations were based on the two case studies described earlier. The HFHS-day1 dataset exemplifies a scenario, with a large number of taxa (558) and a small number of samples (47), while the CD dataset represents the opposite scenario, with a large number of samples (975) and a moderate number of taxa (48 genera). The simulation process, described in Figures 2 and 3, starts from the original microbiome table, **D**, a matrix of counts or proportions with *n* rows (samples) and *C* columns (taxa).

For each simulation scenario, the abundance table **X** was obtained by randomly selecting *k* columns (taxa) from the original dataset **D**. The first k_1 columns of **X** were used to generate the binary response *Y* (as described later) and are thus associated with the outcome, while the remainder $k_2 = k - k_1$ taxa are not associated with the outcome (since they are not used to simulate *Y*). The number of taxa associated with the outcome was $k_1 \in \{3, 5, 10\}$. This subset of variables is denoted by K_1. The number of taxa non-associated with the outcome, denoted by K_2, was $k_2 \in \{10, 20, 30, 40\}$ for the simulations based on the CD dataset and $k_2 \in \{100, 200, 300, 400\}$ for the simulations based on the HFHS-day1 dataset.

We considered two different schemes for generating the dependent variable *Y*: a parametric approach based on a log-contrast model and a non-parametric approach based on *K*-means method (Figure 3). In the parametric approach, we considered a logistic model with a log-contrast linear regression term by taking the log-transformed K_1 variables as covariates and regression coefficients restricted to have a sum equal to zero. This constraint accommodates for the compositional structure of the simulated data. This simulation scheme may favor methods with a similar log-contrast structure such as *coda-lasso* or *selbal*. Therefore, we considered a non-parametric simulation scheme based on *K*-means that consists in calculating the Aitchison distance of the samples using only the K_1 variables, and performing a *K*-means clustering method with two clusters. This process identifies two groups of samples according to the K_1 taxa abundance profile, where samples within the same group have similar profiles while samples in distinct groups are more different. Samples belonging to cluster 1 were as-
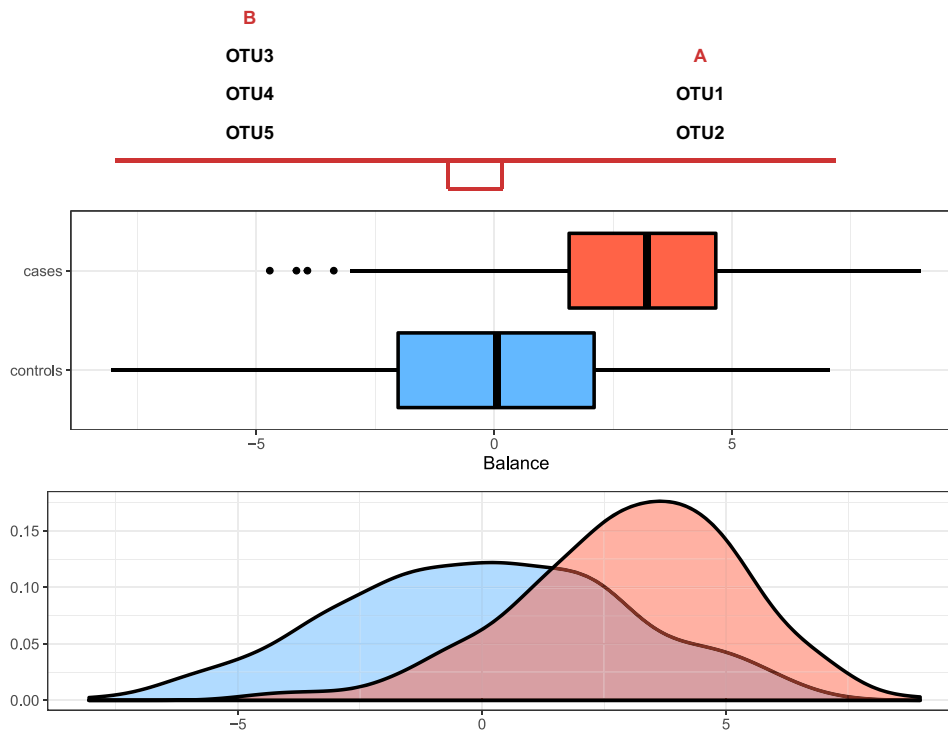
Figure 1. The taxa in group *A* and group *B* that constitute the balance. Box plots represent the distribution of balance scores for cases (red) and controls (blue). The density plot of balance scores for cases and controls is shown below.

signed $Y = 0$ and those belonging to cluster 2 were assigned $Y = 1$. Thus, this process constructs a dependent variable Y that is associated with the K_1 taxa without using a specific parametric model. A detailed description of the simulation scheme is provided in the Supplementary Data. In total, we generated 48 simulated scenarios (2 datasets × 2 methods for generating Y × 3 K_1 subsets of taxa associated with the outcomes × 4 K_2 subsets of non-relevant taxa) that were repeated a hundred times each.

For the three methods, the number of selected variables was determined according to the maximization of the proportion of explained deviance. Methods were then assessed based on the true positive rate (TPR = proportion of associated taxa among the selected variables) and the false positive rate (FPR = proportion of non-associated taxa among the selected variables). These proportions depend on the total number of variables selected by each method, i.e. the penalization parameter λ for *clr-lasso* and *coda-lasso*. When $\lambda = 0$, no penalization is applied and all variables are selected; thus, TPR = FPR = 1. When λ is large, no variables are selected and TPR = FPR = 0. We assessed *clr-lasso* and *coda-lasso* for a sequence of values of $\lambda \in \{0, 0.1, 0.2, \ldots, 1\}$ and then obtained TPR(λ) and FPR(λ). The points $(1 - \text{FPR}(\lambda), \text{TPR}(\lambda))$ represent the ROC curve and the AUC provides a summary measure of the accuracy of each method. For *selbal*, we measured the proportion of true positives and true negatives as a function of the number of selected variables at every step of the forward selection process, and then calculated the AUC of the ROC curve defined by $(1 - \text{FPR}(nvar), \text{TPR}(nvar))$ for $nvar \in \{2, 3, 4, 5, \ldots, \max V\}$.

RESULTS

High-fat high-sugar diet in mice

As already described in other studies, e.g. (43), a change from normal to HFHS diet in mice causes rapid alterations in microbiome composition. This was also the case in the HFHS-day1 study, where we observed a strong association between microbiome composition and diet. *Selbal* identified two taxa whose log ratio perfectly discriminated the two groups of mice (AUC = 1, Figure 4). While *selbal* was able to achieve maximum discrimination with only 2 taxa, *coda-lasso* required at least 7 taxa and *clr-lasso* at least 17 to obtain 100% of explained deviance. For comparison purposes, we set the penalty term for *clr-lasso* to select 10 taxa (corresponding to 95% of explained deviance). Four variables were selected by both *coda-lasso* and *clr-lasso*, while the two variables selected by *selbal* were in common either with *clr-lasso* or with *coda-lasso* (Figure 5).

Most of the bacteria selected by *clr-lasso* were within the order *Clostridiales* (7 out of 10) from the families *Lachnospiraceae*, *Mogibacteriaceae* and *Ruminococcaceae*. These families have been found to be associated with high-fat and/or high-sugar diet in mice (44–47). Corroborating these studies, we also found that the relative abundance of *Lachnospiraceae* was increased in the mice fed with HFHS diet compared to normal diet. *Lachnospiraceae* consists of pro-inflammatory bacteria (47), which are also reported to be associated with chronic inflammation of the gut (48,49).

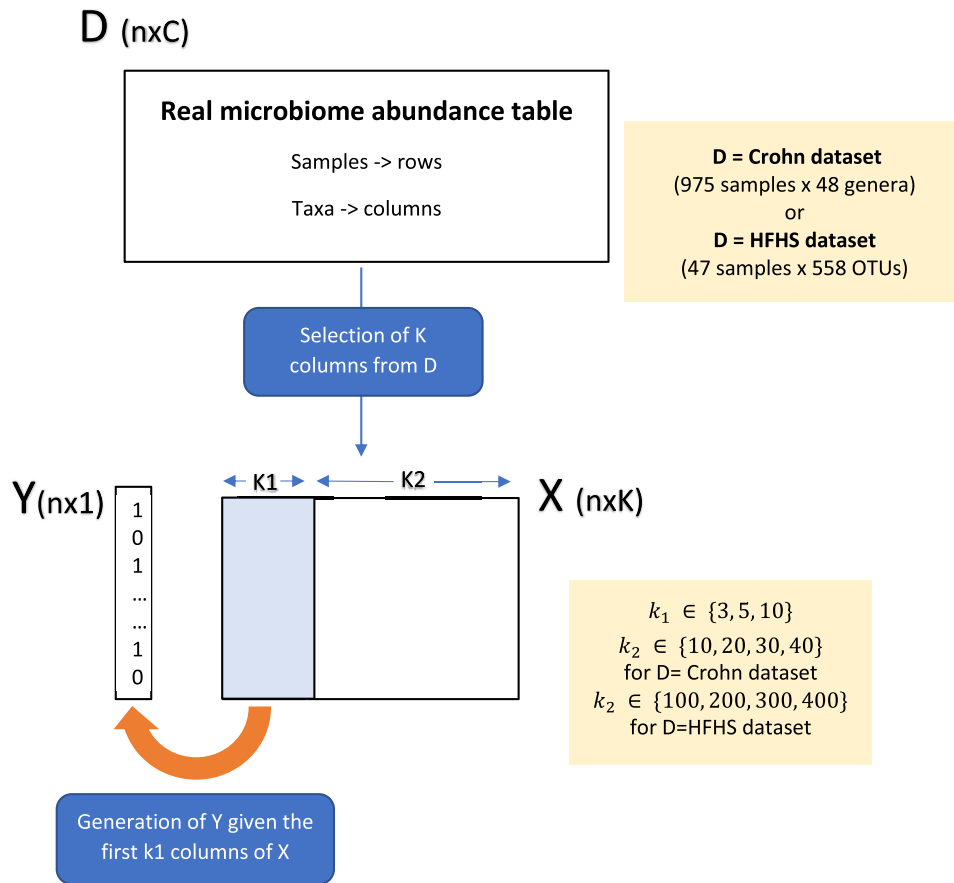The taxa selected by *coda-lasso* belonged to the order *Bacteroidales* (6 out of 7) including the family *S24-7* (5

Figure 2. Simulation scheme: the simulated abundance table **X** is obtained by randomly selecting k columns from the original dataset **D**. The first k_1 columns of **X** are used to generate the binary response Y, while the remainder k_2 taxa are deemed irrelevant to explain the outcome. The sizes of K_1 and K_2 vary depending on **D**.
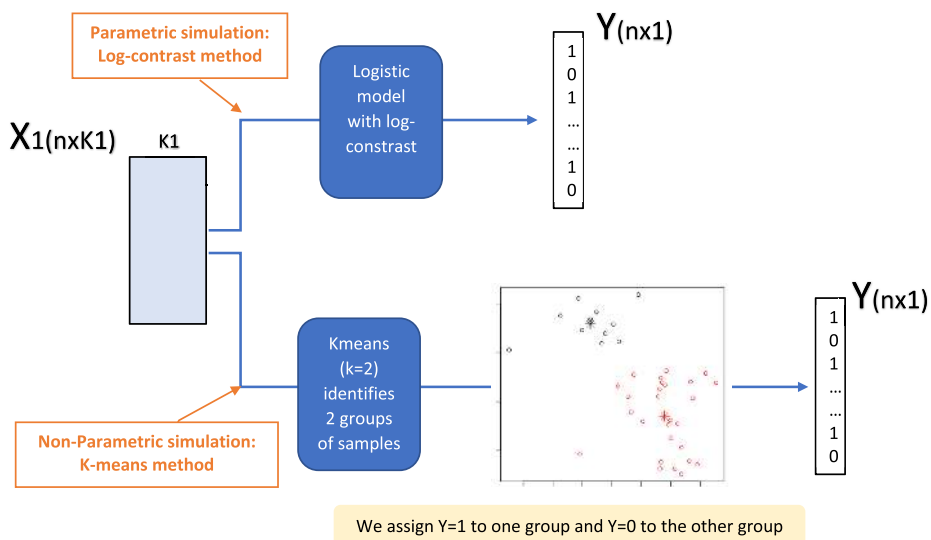
Figure 3. Two schemes were used to generate Y given the K_1 taxa, using a parametric method based on log contrasts, or a non-parametric approach based on K-means.
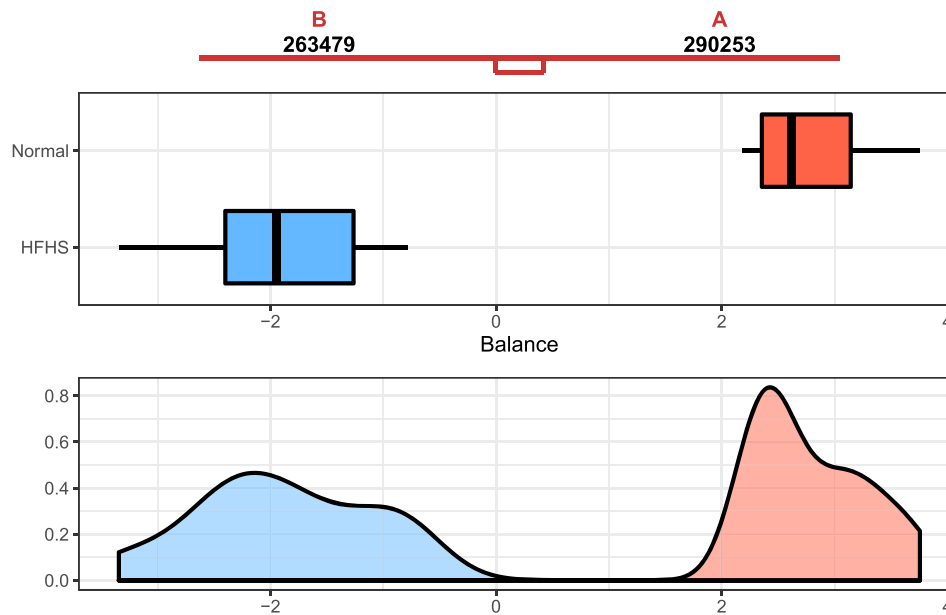
Figure 4. Representation of the distribution of balance values (log ratio) between the two taxa selected by *selbal* (OTUs 290253 *g_Oscillospira* and 263479 *o_Bacteroidales; f_s24–7*) for the mice on an HFHS diet (blue) or normal diet (red) in the HFHS-day1 whole dataset.
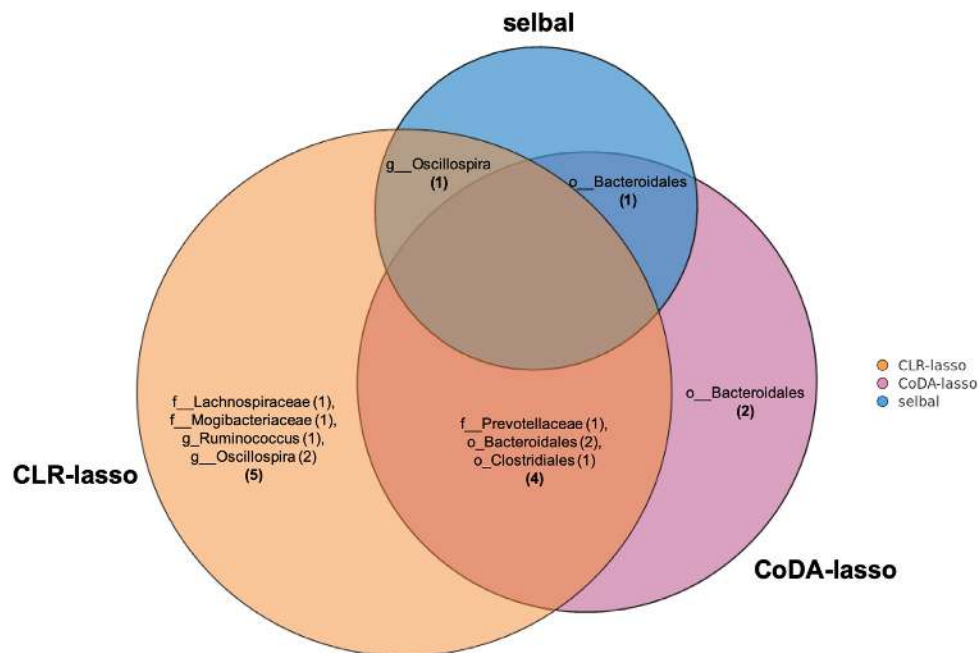

Figure 5. Concordance of the taxa selected by the three methods *selbal* (blue), *clr-lasso* (orange) and *coda-lasso* (pink) for the HFHS-day1 dataset (o = order, f = family and g = genera are indicated depending on available taxonomy).

out of 6) and Prevotellaceae. The abundance of *S24-7* was found to be increased in the diabetes-sensitive mice fed with a high-fat diet, especially after the treatment of remitting colitis in mice (50), while in normal mice, a high-fat diet reduced the abundance of *S24-7*, which was negatively associated with the inflammatory mediator IL-6 (51). Family Prevotellaceae is able to ferment carbohydrate and protein and was found abundant in obese human individuals (52). In our analysis, the relative abundance of these two fami-

lies was found to be increased in HFHS diet compared to normal diet.

Selbal selected the genus *Oscillospira* from order *Clostridiales* overlapping with *clr-lasso*, and an unclassified genus from order *Bacteroidales* overlapping with *coda-lasso*.

Though *selbal* selects only two taxa, we emphasize that other taxa are also highly associated with diet in this study. Indeed, in an $n \ll k$ setting, it is highly probable that a given

balance is not unique and alternative microbial signatures may provide similar results. We investigated other balances by removing the two selected taxa from the dataset and performing *selbal* again. The method identified a second pair of taxa also with maximum accuracy (AUC = 1 and 100% of explained deviance). The two new selected taxa were both among the variables selected by *clr-lasso* and one of them among the selected variables by *coda-lasso*. This case study illustrates the main difference between the methods: *selbal* seeks for the most parsimonious model with maximum prediction or classification accuracy, while the complexity (i.e. number of variables selected) of *clr-lasso* and *coda-lasso* is determined by the penalization parameter. Though penalized regression models are useful for the identification of the variables that are most associated with the outcome, they do not guarantee the best classification performance.

Crohn's disease

In previous analysis of this dataset with *selbal*, a balance with 12 variables was determined optimal to discriminate the CD status (26). For ease of comparison, we specified penalized parameters that resulted in the selection of 12 variables for both *coda-lasso* and *clr-lasso*. The optimization criterion for fitting the models was the maximization of the proportion of deviance explained.

The microbial signature that best discriminates between CD and controls according to *selbal* is given by the balance between taxa in group $A = \{o\_Clostridiales\_g\_,$ $g\_Bacteroides,$ $f\_Peptostreptococcaceae\_g\_,$ $g\_Roseburia\}$ and taxa in group $B = \{g\_Blautia,$ $g\_Oscillospira,$ $g\_Dorea,$ $g\_$ $Adlercreutzia,$ $g\_Streptococcus,$ $g\_Dialister,$ $g\_Eggerthella,$ $g\_Aggregatibacter,$ $g\_Adlercreutzia\}$. The average abundance (geometric mean) of taxa in group A relative to group B is larger in controls than in CD patients (Figure 6).

Figure 7 describes the taxa that were selected by the three methods: six taxa in common, seven taxa identified by two methods, two taxa selected solely by *selbal* and two taxa only by *coda-lasso*. All the taxa selected by any of the methods have been previously described as markers of inflammation and dysbiosis in CD (41,53–55).

Although the number of variables selected by the three methods was the same, the proportion of explained deviance was considerably larger for *selbal* (27%) than for *clr-lasso* (18%) and *coda-lasso* (21%).

To further assess the classification performance of each method and which taxa signature might be best, we implemented 5-fold cross-validation repeated 20 times, where the signature identified in each training fold was then tested to predict disease status on the test dataset. For each model, or microbial signature, we calculated the ROC curve and the AUC to measure its classification or discrimination accuracy (Figure 8). *Selbal* microbial signatures led to slightly better classification accuracy than *clr-lasso* and *coda-lasso*, which resulted in similar performance.

SIMULATION STUDY

The results of all simulation scenarios are summarized in terms of mean AUC in Figure 9 (simulations based on

the CD dataset) and Figure 10 (simulations based on the HFHS-day1 dataset). As expected, we observed a better performance of all methods for the $n \gg k$ case (CD dataset) than for the $n \ll k$ case (HFHS-day1). In particular, we observed a decrease in performance accuracy when the number of taxa associated with the outcome increased. This can be explained as for a fixed joint effect, the larger the number of discriminant taxa, the smaller their individual contribution.

The performance of the methods is highly dependent on the total number of variables in the dataset. In the $n \ll k$ scenario (Figure 10), we observed a small decrease in performance of all methods as the total number of variables increases from $k_1 + 100$ to $k_1 + 400$, with $k_1 \in \{3, 5, 10\}$. In the $n \gg k$ scenario (Figure 9), both *selbal* and *coda-lasso* had a stable performance as the number of variables increased from $k_1 + 10$ to $k_1 + 40$. However, we observed a distinct behavior of *clr-lasso*: its performance was poor for a small number of variables ($k_1 + 10$ and $k_1 + 20$) but improved when k increased. This can be explained by the instability introduced by the clr transformation. Since, $\text{clr}(x_{ji}) = \log(x_{ji}) - M_i$, for taxa j and sample i, the variability of M reduces the power to detect a possible association between the response Y and taxa j. However, as the total number of taxa k increases, the variability of M, given by

$$\text{var}(M) = \frac{1}{k^2} \left(\sum_{j=1}^{k} \text{var}(\log(x_j)) + 2 \sum_{l,j=1; l \neq j}^{k} \text{covar}(\log(x_l), \log(x_j)) \right), \quad (19)$$

is likely to decrease for large values of k because the term k^2 in the denominator dominates the numerator in $\text{var}(M)$. This is the case, for instance, in the $n \ll k$ scenario where the variability of M tends to zero when the total number of variables increases (Figure 11). We also observed similar behavior for the HFHS dataset (data not shown).

DISCUSSION

Variable selection is one of the key procedures in microbiome data analysis. It is relevant for the identification of microbial species that are involved in biological processes or when the interest is the detection of microbial signatures that can serve as biomarkers of disease risk and prognostic (56). The first goal improves biological knowledge and requires precise estimations and control of TPR and FPR. The second goal focuses on classification and prediction: different models can lead to similar prediction accuracy, but parsimonious models can be preferred for their translational use as microbial signatures. It is worth noting that no method can be optimal for both aims.

In this work, we compared three approaches for variable selection in microbiome studies that follow the principles of CoDA, either by considering balances of groups of taxa associated with the outcome (*selbal*) or with penalized regression after clr transformation (*clr-lasso*) or constraints on the regression coefficients (*coda-lasso*). The interpretation of the results is not straightforward in a compositional framework, and we provided practical advice to apply and
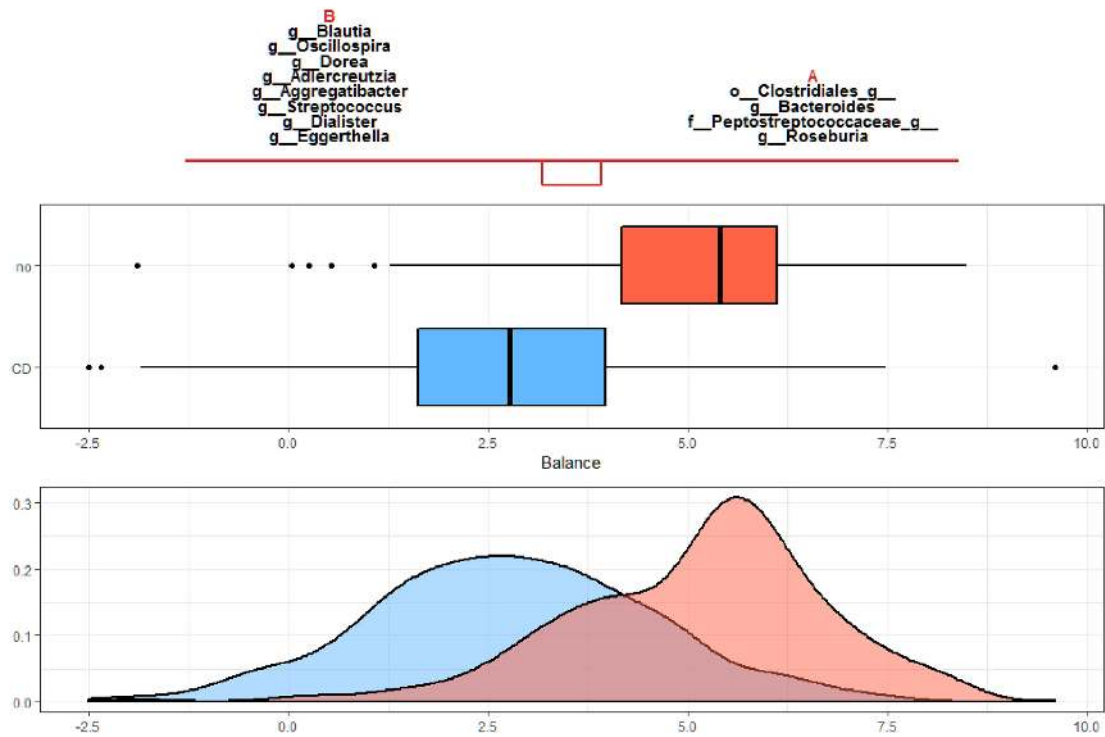
Figure 6. Representation of the distribution of balance values (log ratio) between the geometric means of the two taxa groups selected by *selbal* for CD (blue) and controls (red) in the CD whole dataset.
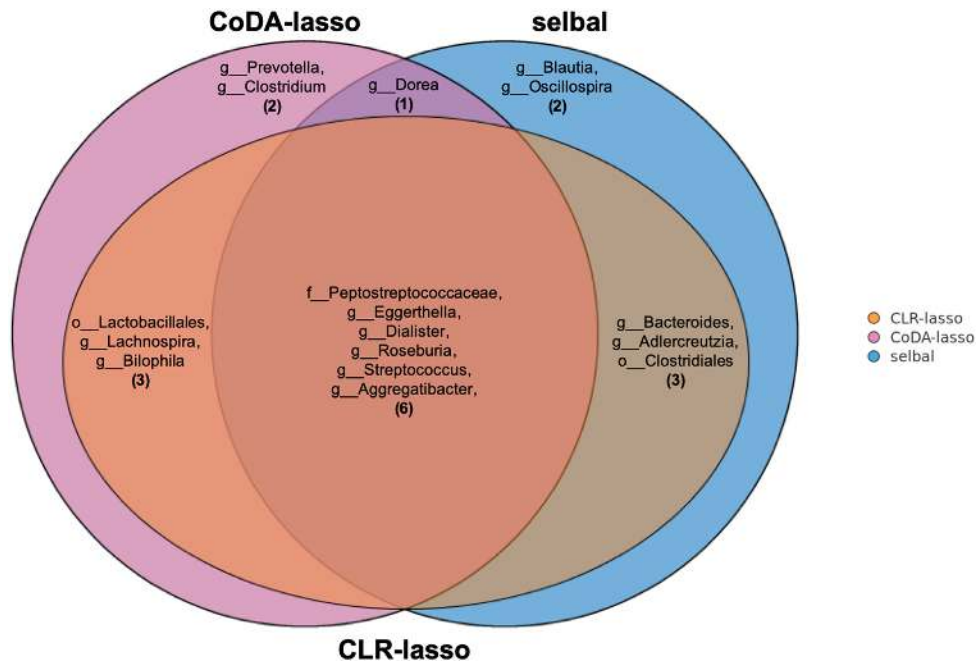

Figure 7. Concordance of the selected taxa for the CD dataset by the three methods considered: *selbal* (blue), *clr-lasso* (orange) and *coda-lasso* (pink) (f = family; g = genera).
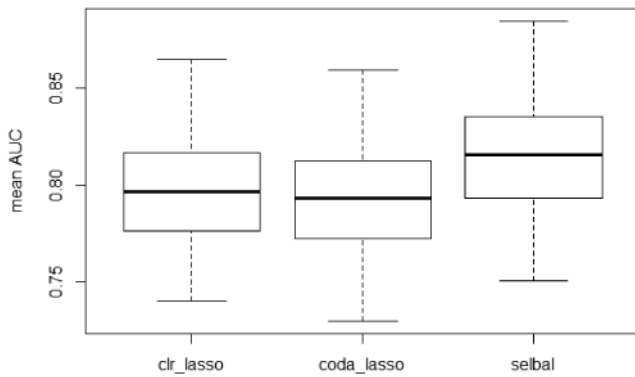
Figure 8. Box plot of the mean AUC of the cross-validation process to evaluate the classification accuracy of *clr-lasso*, *coda-lasso* and *selbal* on the CD dataset.

make sense of the results obtained. In addition, we discussed the different objectives of the approaches we considered. *Selbal*'s main goal is the establishment of microbial signatures with predictive ability to be used as diagnostic or prognostic markers and thus prioritizes parsimonious models. Penalized regression models seek for the identification of microbial species that in combination relate to the phenotype of interest to increase biological knowledge of the link between disease and microbiome.

Selbal identifies two groups of bacteria whose relative average abundance is associated with the outcome. Such approach is well suited to how we describe microbiome–disease associations in terms of dysbiosis or imbalance be-

tween beneficial and pathogenic microbes. In our case studies, *Selbal* led to better performance than the penalized approaches. In the HFHS dataset, *selbal* only needed 2 variables to achieve maximum discrimination, while *coda-lasso* and *clr-lasso* required 7 and 17, respectively. In the CD dataset, *selbal* model explained a larger proportion of explained variance and led to slightly higher classification accuracy compared to the other approaches, based on the same selection size. These results can be explained by either a better selection of the features that constitute the signature or the way the microbial signatures are calculated after variable selection. While *clr-lasso* and *coda-lasso* regression coefficients are estimated from the training dataset, *selbal* only retains the set of selected variables and the sign of the coefficients, and each regression coefficient is given by the inverse of the number of variables with either positive or negative sign. Our simulated results suggest that the estimation of coefficients with penalized regression may lead to some overfitting and thus a worse performance than *selbal*. While this approach is suited for the identification of a predictive microbial signature, it comes with computational cost because of the forward selection process. We propose to apply a combination of *selbal* with one of the two penalized regression methods to filter the number of variables and lessen the computational burden. This, however, should be done carefully using cross-validation to avoid variable selection bias.

Penalized regression after clr transformation is a valid CoDA approach, but we have identified important drawbacks. Clr penalized regression is not subcompositionally consistent, meaning that different subcompositions will rise
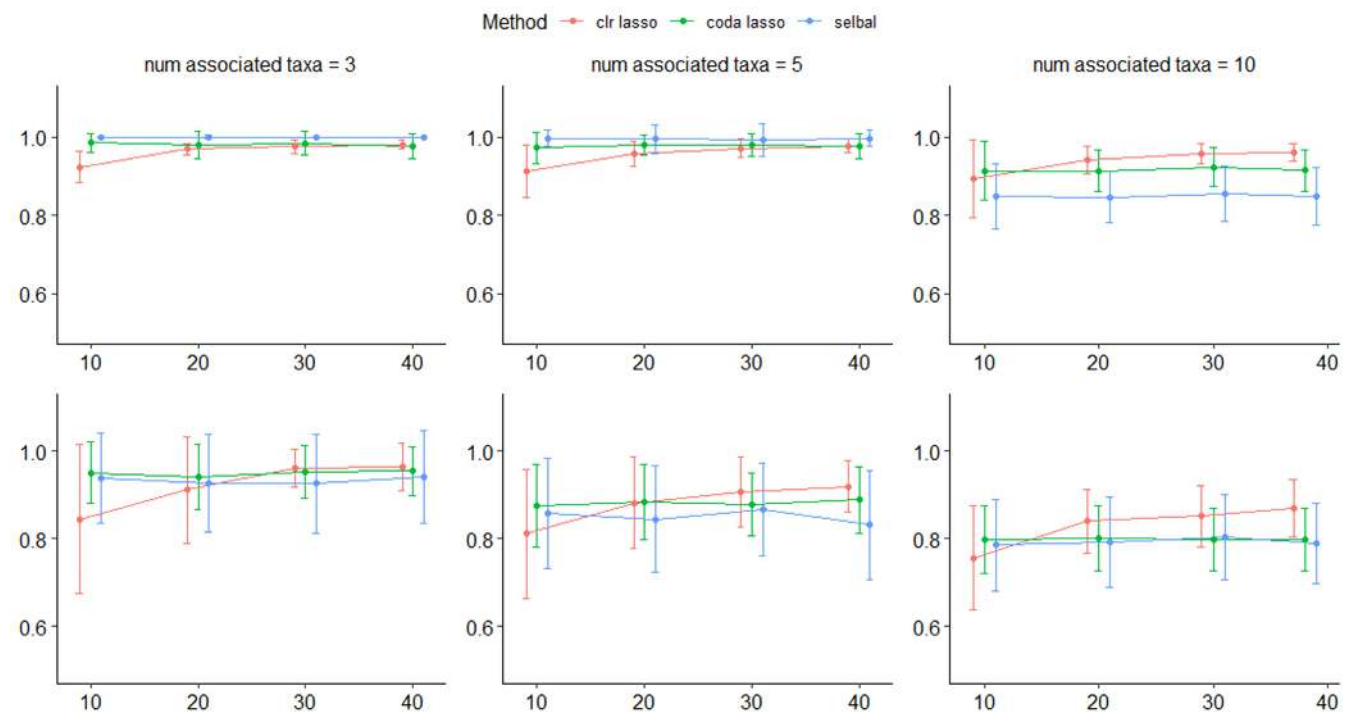

Figure 9. Mean AUC for variable selection in the simulations based on the CD dataset for *selbal* (blue), *clr-lasso* (red) and *coda-lasso* (green). The first row corresponds to the log-contrast method to generate Y and the second row to the K-means method. The three columns correspond to the number of taxa associated with Y, $k_1 \in \{3, 5, 10\}$, and the x-axis specifies the number of non-associated taxa, $k_2 \in \{10, 20, 30, 40\}$.
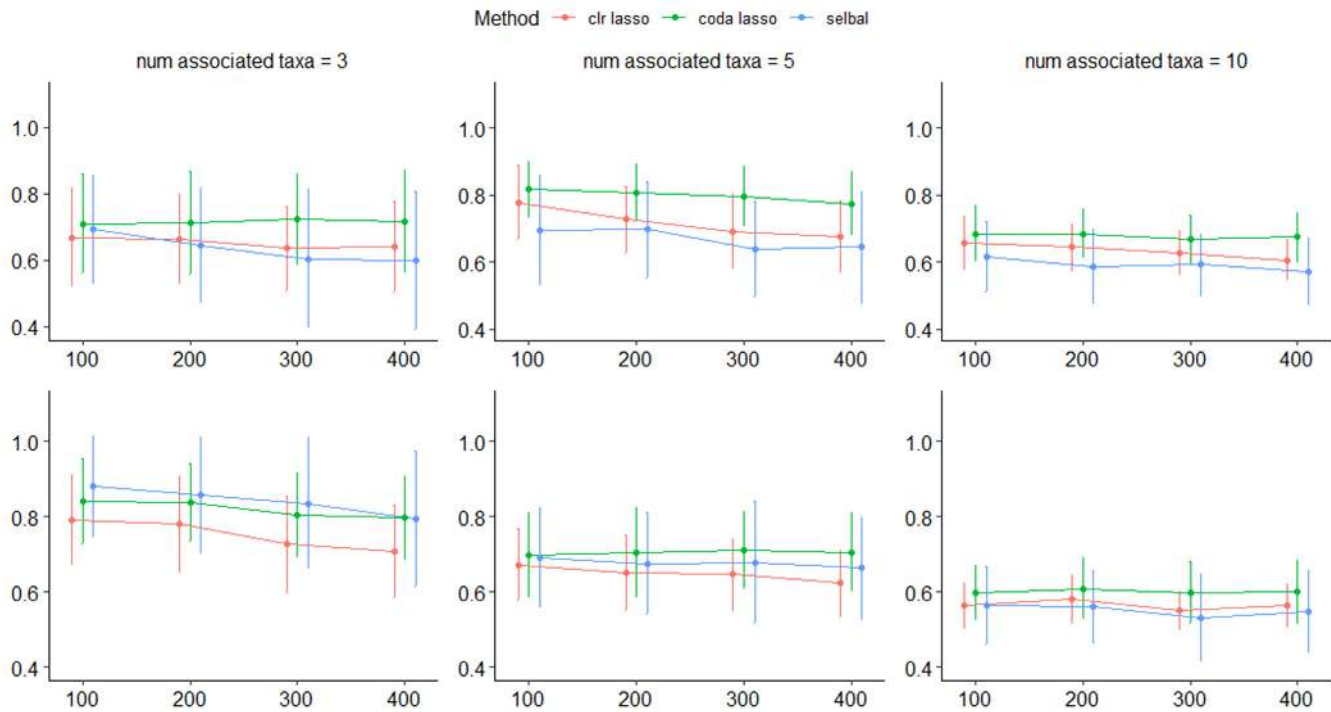
Figure 10. Mean AUC for variable selection in the simulations based on the HFHS dataset for *selbal* (blue), *clr-lasso* (red) and *coda-lasso* (green). The first row corresponds to the log-contrast method to generate Y and the second row to the K-means method. The three columns correspond to the number of taxa associated with Y, $k_1 \in \{3, 5, 10\}$, and the x-axis specifies the number of non-associated taxa, $k_2 \in \{100, 200, 300, 400\}$.
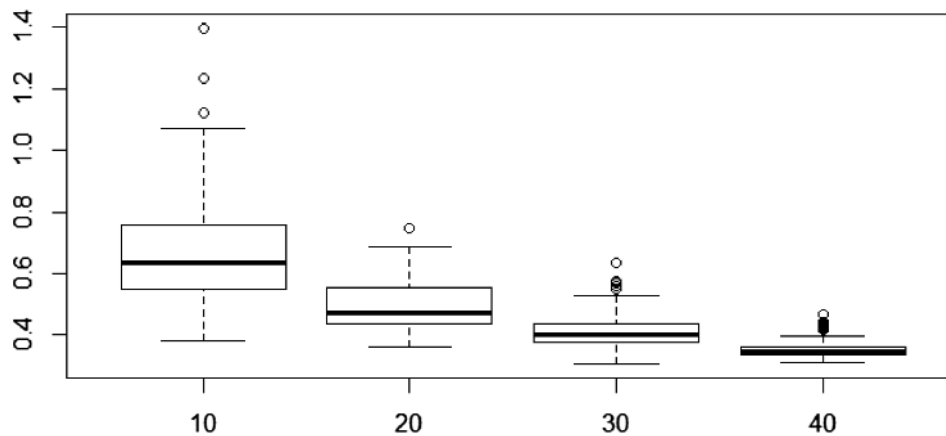

Figure 11. Variability of M after clr transformation [see Equation (19)] for the $n \gg k$ scenario, based on the CD dataset. The total number of variables for each simulation scheme is indicated in the x-axis.

to different transformations of the data. Therefore, results are not readily transferable from one study to another where different filtering processes were performed. In addition, microbial signatures obtained from this approach can be difficult to implement on an independent dataset as it raises the question of how the variable from the new dataset should be clr-transformed, and based on which components. The new dataset may include different components, e.g. new taxa not detected in the previous dataset. Most importantly, irrelevant variables are not entirely removed from the analysis: we have shown that all variables remain in the clr transformation term (the geometric mean of all clr-transformed variables).

Clr transformation is algebraically very similar to *edgeR* and *DeSeq2* normalization techniques (57), which suggests that it can be used as library size normalization. However, normalization alone does not solve the compositional issue; thus, univariate testing of clr-transformed variables may result in high FPR when the composition abundances between samples are markedly different.

Using the terminology by Morton *et al.* (24), the clr transformation uses all taxa as the 'reference frame'. Such reference may not be suitable in our context as it combines both taxa that are rather stable and taxa that might be quite variable across experimental conditions. The adverse impact of using all taxa as a reference is more evident when

the number of taxa is small, as we showed in our simulation study. When $n \gg k$, the clr transformation introduces noise and reduces power to detect real associations. When $n \ll k$, the clr transformation reduces to an almost constant shift and the analysis is very similar to an analysis of the log-transformed data without any CoDA consideration.

Penalized regression with coefficients restricted to a sum equal to zero, *coda-lasso*, is an elegant and appropriate CoDA approach. Computation time is efficient and the results can be interpreted as balances between two groups of taxa with weights. However, the determination of the penalty parameter (i.e. the number of variables to retain in the model) is a limitation in this approach. *Coda-lasso* is suitable to identify variables that are most associated with the outcome though it does not necessary lead to the best accuracy nor the most parsimonious model.

Though not addressed in this work, it is worth noting that, as any CoDA approach, the methods we have assessed rely on logarithms and require handling of zeros. The proportion and nature of the zeros in the dataset will determine the treatment of zeros and also the performance of variable selection methods.

To conclude, users should choose the method that best fits their needs and analysis objectives. Regardless of the approach chosen, we emphasize that variable selection in microbiome studies should be conducted with a multivariate approach that accounts for compositional characteristics, and that the interpretation of the associations of the microbiome with the response variable should be done in terms of balances between groups of bacteria.

SUPPLEMENTARY DATA

Supplementary Data are available at NAR Online.

FUNDING

REFERENCES

1. Calle,M.L. (2019) Statistical analysis of metagenomics data. *Genomics Inform.* **17**, e6.
2. Gloor,G.B., Macklaim,J.M., Pawlowsky-Glahn,V. and Egozcue,J.J. (2017) Microbiome datasets are compositional: and this is not optional. *Front. Microbiol.*, **8**, 2224.
3. Thorsen,J., Brejnrod,A., Mortensen,M., Rasmussen,M.A., Stokholm,J., Al-Soud,W.A., Sørensen,S., Bisgaard,H. and Waage,J. (2016) Large-scale benchmarking reveals false discoveries and count transformation sensitivity in 16S rRNA gene amplicon data analysis methods used in microbiome studies. *Microbiome*, **4**, 62.
4. Hibbing,M.E., Fuqua,C., Parsek,M.R. and Peterson,S.B. (2010) Bacterial competition: surviving and thriving in the microbial jungle. *Nat. Rev. Microbiol.*, **8**, 15–25.
5. Gloor,G.B., Wu,J.R., Pawlowsky-Glahn,V. and Egozcue,J.J. (2016) It's all relative: analyzing microbiome data as compositions. *Ann. Epidemiol.*, **26**, 322–329.
6. Gloor,G.B. and Reid,G. (2016) Compositional analysis: a valid approach to analyze microbiome high-throughput sequencing data. *Can. J. Microbiol.*, **62**, 692–703.
7. Quinn,T.P., Erb,I., Gloor,G., Notredame,C., Richardson,M.F. and Crowley,T.M. (2019) A field guide for the compositional analysis of any-omics data. *GigaScience*, **8**, giz107.
8. Weiss,S., Xu,Z.Z., Peddada,S., Amir,A., Bittinger,K., Gonzalez,A., Lozupone,C., Zaneveld,J.R., Vázquez-Baeza,Y., Birmingham,A. *et al.* (2017) Normalization and microbial differential abundance strategies depend upon data characteristics. *Microbiome*, **5**, 27.
9. Segata,N., Izard,J., Waldron,L., Gevers,D., Miropolsky,L., Garrett,W.S. and Huttenhower,C. (2011) Metagenomic biomarker discovery and explanation. *Genome Biol.*, **12**, R60.
10. Paulson,J.N., Stine,O.C., Bravo,H.C. and Pop,M. (2013) Differential abundance analysis for microbial marker-gene surveys. *Nat. Methods*, **10**, 1200–1202.
11. Robinson,M.D., McCarthy,D.J. and Smyth,G.K. (2010) edgeR: a Bioconductor package for differential expression analysis of digital gene expression data. *Bioinformatics*, **26**, 139–140.
12. Love,M.I., Huber,W. and Anders,S. (2014) Moderated estimation of fold change and dispersion for RNA-seq data with DESeq2. *Genome Biol.*, **15**, 550.
13. Robinson,M.D. and Oshlack,A. (2010) A scaling normalization method for differential expression analysis of RNA-seq data. *Genome Biol.*, **11**, R25.
14. Anderson,M.J. (2001) A new method for non-parametric multivariate analysis of variance. *Austral Ecol.*, **26**, 32–46.
15. Clarke,K.R. (1993) Non-parametric multivariate analyses of changes in community structure. *Aust. J. Ecol.*, **18**, 117–143.
16. La Rosa,P.S., Brooks,J.P., Deych,E., Boone,E.L., Edwards,D.J., Wang,Q., Sodergren,E., Weinstock,G. and Shannonet,W.D. (2012) Hypothesis testing and power calculations for taxonomic-based human microbiome data. *PLoS One*, **7**, e52078.
17. Lê Cao,K.-A., Costello,M., Lakis,V.A., Bartolo,F., Chua,X., Brazeilles,R. and Rondeau,P. (2016) MixMC: a multivariate statistical framework to gain insight into microbial communities. *PLoS One*, **11**, e0160169.
18. Mandal,S., Van Treuren,W., White,R.A., Eggesbo,M., Knight,R. and Peddada,S.D. (2015) Analysis of composition of microbiomes: a novel method for studying microbial composition. *Microb. Ecol. Health Dis.*, **26**, 27663.
19. Fernandes,A.D., Macklaim,J.M., Linn,T.G., Reid,G. and Gloor,G.B. (2013) ANOVA-like differential expression (ALDEx) analysis for mixed population RNA-Seq. *PLoS One*, **8**, e67019.
20. Pawlowsky-Glahn,V., Egozcue,J.J. and Tolosana-Delgado,R. (2011) Principal balances. In: *Proceedings of the 4th International Workshop on Compositional Data Analysis(CODAWORK)*.
21. Morton,J.T., Sanders,J., Quinn,R.A., McDonald,D., Gonzalez,A., Vázquez-Baeza,Y., Navas-Molina,J.A., Song,S.J., Metcalf,J.L., Hyde,E.R. *et al.* (2017) Balance trees reveal microbial niche differentiation. *mSystems*, **2**, e00162-16.
22. Silverman,J.D., Washburne,A.D., Mukherjee,S. and David,L.A. (2017) A phylogenetic transform enhances analysis of compositional microbiota data. *eLife*, **6**, e21887.
23. Washburne,A.D., Silverman,J.D., Leff,J.W., Bennett,D.J., Darcy,J.L., Mukherjee,S., Fierer,N. and David,L.A. (2017) Phylogenetic factorization of compositional data yields lineage-level associations in microbiome datasets. *PeerJ*, **5**, e2969.
24. Morton,J.T., Marotz,C., Washburne,A., Silverman,J., Zaramela,L.S., Edlund,A., Zengler,K. and Knight,R. (2019) Establishing microbial composition measurement standards with reference frames. *Nat. Commun.*, **10**, 2719.
25. Quinn,T.P. and Erb,I. (2019) Using balances to engineer features for the classification of health biomarkers: a new approach to balance selection. bioRxiv doi: https://doi.org/10.1101/600122, 1 May 2019, preprint: not peer reviewed.
26. Rivera-Pinto,J., Egozcue,J.J., Pawlowsky-Glahn,V., Paredes,R., Noguera-Julian,M. and Calle,M.L. (2018) Balances: a new perspective for microbiome analysis. *mSystems*, **3**, e00053-18.
27. Tibshirani,R. (1996) Regression shrinkage and selection via the lasso. *J. R. Stat. Soc. Ser. B: Stat. Methodol.*, **58**, 267–288.

28. Cessie,S.L. and Houwelingen,J.C.V. (1992) Ridge estimator in logistic regression. *J. R. Stat. Soc. Ser. C: Appl. Stat.*, **41**, 191–201.

29. Zou,H. and Hastie,T. (2005) Regularization and variable selection via the elastic net. *J. R. Stat. Soc. Ser. B: Stat. Methodol.*, **67**, 301–320.

30. Lin,W., Shi,P., Feng,R. and Li,H. (2014) Variable selection in regression with compositional covariates. *Biometrika*, **101**, 785–797.

31. Lu,J., Shi,P. and Li,H. (2018) Generalized linear models with linear constraints for microbiome compositional data. *Biometrics*, **75**, 235–244.

32. Aitchison,J. (1986) *The Statistical Analysis of Compositional Data*. Chapman & Hall, London.

33. Pawlowsky-Glahn,V., Egozcue,J.J. and Tolosana-Delgado,R. (2015) *Modelling and Analysis of Compositional Data*. Wiley, NY.

34. Egozcue,J.J., Pawlowsky-Glahn,V., Mateu-Figueras,G. and Barceló-Vidal,C. (2003) Isometric logratio transformations for compositional data analysis. *Math. Geol.*, **35**, 279–300.

35. Greenacre,M., Grunsky,E.C. and Bacon-Shone,J. (2019) A comparison of amalgamation and isometric logratios in compositional data analysis. ResearchGate https://www.researchgate.net/publication/332656109, 11 May 2020, preprint: not peer reviewed.

36. Carding,S., Verbeke,K., Vipond,D.T., Corfe,B.M. and Owen,L.J. (2015) Dysbiosis of the gut microbiota in disease. *Microb. Ecol. Health Dis.*, **26**, 26191.

37. Sheflin,A.M., Whitney,A.K. and Weir,T.L. (2014) Cancer-promoting effects of microbial dysbiosis. *Curr. Oncol. Rep.*, **16**, 406.

38. Aitchison,J. and Bacon-Shone,J. (1984) Log contrast models for experiments with mixtures. *Biometrika*, **71**, 323–330.

39. van den Boogaart,K.G. and Tolosana-Delgado,R. (2008) "Compositions": a unified R package to analyze compositional data. *Comput. Geosci.*, **34**, 320–338.

40. Friedman,J., Hastie,T. and Tibshirani,R. (2010) Regularization paths for generalized linear models via coordinate descent. *J. Stat. Softw.*, **33**, 1–22.

41. Gevers,D., Kugathasan,S., Denson,L.A., Vázquez-Baeza,Y., Van Treuren,W., Ren,B., Schwager,E., Knights,D., Song,S.J., Yassour,M. *et al.* (2014) The treatment-naïve microbiome in new-onset Crohn's disease. *Cell Host Microbe*, **15**, 382–392.

42. Gonzalez,A., Navas-Molina,J.A., Kosciolek,T., McDonald,D., Vázquez-Baeza,Y., Ackermann,G., DeReus,J., Janssen,S., Swafford,A.D., Orchanian,S.B. *et al.* (2018) Qiita: rapid, web-enabled microbiome meta-analysis. *Nat. Methods*, **15**, 796–798.

43. Hildebrandt,M., Hoffmann,C., Sherrill-Mix,S.A., Keilbaughlow,S.A., Hamady,M., Chenlow,Y., Knight,R., Ahima,R.S., Bushman,F. and Wu,G.D. (2009) High-fat diet determines the composition of the murine gut microbiome independently of obesity. *Gastroenterology*, **137**, 1716–1724.

44. Zhao,R., Khafipour,E., Sepehri,S., Huang,F., Beta,T. and Shen,G.X. (2019) Impact of Saskatoon berry powder on insulin resistance and relationship with intestinal microbiota in high fat–high sucrose diet-induced obese mice. *J. Nutr. Biochem.*, **69**, 130–138.

45. Muhomah,T.A., Nishino,N., Katsumata,E., Haoming,W. and Tsuruta,T. (2019) High-fat diet reduces the level of secretory immunoglobulin A coating of commensal gut microbiota. *Biosci. Microbiota Food Health*, **38**, 55–64.

46. Sanguinetti,E., Collado,M.C., Marrachelli,V.G., Monleon,D., Selma-Royo,M., Pardo-Tendero,M.M, Burchielli,S. and Iozzo,P. (2018) Microbiome-metabolome signatures in mice genetically prone to develop dementia, fed a normal or fatty diet. *Sci. Rep.*, **8**, 4907.

47. Voigt,R.M., Forsyth,C.B., Green,S.J., Mutlu,E., Engen,P., Vitaterna,M.H. and Turek,F.W. (2014) Circadian disorganization alters intestinal microbiota. *PLoS One*, **9**, e97500.

48. Zeng,H., Ishaq,S.L., Zhao,F.Q. and Wright,A.D.G. (2016) Colonic inflammation accompanies an increase of β-catenin signaling and Lachnospiraceae/Streptococcaceae bacteria in the hind gut of high-fat diet-fed mice. *J. Nutr. Biochem.*, **35**, 30–36.

49. Kläring,K., Just,S., Lagkouvardos,I., Hanske,L., Haller,D., Blaut,M., Wenning,M. and Clavel,T. (2015) *Murimonas intestini* gen. nov., sp. nov., an acetate-producing bacterium of the family Lachnospiraceae isolated from the mouse gut. *Int. J. Syst. Evol. Microbiol.*, **65**, 870–878.

50. Ormerod,K.L., Wood,D.L.A., Lachner,N., Gellatly,S.L., Daly,J.N., Parsons,J.D., Dal'Molin,C.G.O., Palfreyman,R.W., Nielsen,L.K., Cooper,M.A. *et al.* (2016) Genomic characterization of the uncultured Bacteroidales family S24-7 inhabiting the guts of homeothermic animals. *Microbiome*, **4**, 36.

51. Pyndt Jørgensen,B., Hansen,J.T., Krych,L., Larsen,C., Klein,A.B., Nielsen,D.S., Josefsen,K., Hansen,A.K. and Sørensen,D.B. (2014) A possible link between food and mood: dietary impact on gut microbiota and behavior in BALB/c mice. *PLoS One*, **9**, e103398.

52. Zhang,H., DiBaise,J.K., Zuccolo,A., Kudrna,D., Braidotti,M., Yu,Y., Parameswaran,P., Crowell,M.D., Wing,R., Rittmann,B.E. *et al.* (2009) Human gut microbiota in obesity and after gastric bypass. *Proc. Natl Acad. Sc. U.S.A.*, **106**, 2365–2370.

53. Shaw,K.A., Bertha,M., Hofmekler,T., Chopra,P., Vatanen,T., Srivatsa,A., Prince,J., Kumar,A., Sauer,C., Zwick,M.E. *et al.* (2016) Dysbiosis, inflammation, and response to treatment: a longitudinal study of pediatric subjects with newly diagnosed inflammatory bowel disease. *Genome Med.*, **8**, 75.

54. Pascal,V., Pozuelo,M., Borruel,N., Casellas,F., Campos,D., Santiago,A., Martinez,X., Varela,E., Sarrabayrouse,G., Machiels,K. *et al.* (2017) A microbial signature for Crohn's disease. *Gut*, **66**, 813–822.

55. Wright,E.K., Kamm,M.A., Teo,S.M., Inouye,M., Wagner,J. and Kirkwood,C.D. (2015) Recent advances in characterizing the gastrointestinal microbiome in Crohn's disease: a systematic review. *Inflamm. Bowel Dis.*, **21**, 1219–1228.

56. Knights,D., Parfrey,L.W., Zaneveld,J., Lozupone,C. and Knight,R. (2011) Human-associated microbial signatures: examining their predictive value. *Cell Host Microbe*, **10**, 292–296.

57. Quinn,T.P., Erb,I., Gloor,G., Richardson,M.F. and Crowley,T.M. (2018) Understanding sequencing data as compositions: an outlook and review. *Bioinformatics*, **34**, 2870–2878.